

Valery SHLYANNIKOV* and Boris ILTCHENKO**

Mixed Mode Fatigue Fracture Taking into Account Inherent Stress Biaxiality in Compact Tension Specimen

* Kazan Power Engineering Institute, Russia

**Kazan Physical - Technical Institute of the Russian Academy of Sciences

Keywords : fatigue, fracture, process zone

ABSTRACT : Previous work by the authors has indicated that crack behaviour in various fracture specimen geometries shows a secondary dependence on the degree of in-plane stress biaxiality. Data published here shows the crack-length dependence of a parameter expressing the degree of stress biaxiality inherent to a two of standard specimen geometries. Through the fracture process zone which develops at the crack tip the influence of the material properties, the shape and size of the single-edge-notched and compact tension specimens on the crack growth rate, shear lips formation and crack front form on different stage of fatigue fracture process was established.

Introduction

In the literature on the fracture mechanic the limitations of the single-parameter theory is discussed. One connects the observed fracture characteristic dependencies on cracked body geometry and its loading conditions with the influence of nonsingular term at small scale yielding. In the notation of Rice (1), the second term in the expansion is denoted the T- stress and can be regarded as a stress parallel to the crack flanks. The magnitude of the T-stress is defined through a biaxially parameter B, introduced by Leever and Radon (2). Larson and Carlsson (3) have shown that the variations in T which have, by manipulating biaxiality of loading, been shown to affect crack behaviour, are encountered in comparing cracks at the same stress intensity factor K loading in different "uniaxially" loaded specimen types. Then Leever and Radon (2) have computed by the finite element method (FEM) the stress biaxiality factor B which is inherent to the standard specimen geometries expressed over the nonsingular term T for elastic and elastic-plastic state conditions. Under fatigue loading the cyclic crack growth rate should be uniquely determined by the K versus time cycle. Some experiments on PMMA, however, have shown that another stress field parameter - one expressing the effective "biaxiality" of the overall stress field - can also influence the crack growth rate.

The transition of tensile-to-shear mode crack growth under uniaxial cyclic tensile stress, leading to the development of shear lips along the edges of the fracture surface in material different properties is a well-known phenomenon. The shear lips can be characterized by the width, the height (Fig. 1) and these dimensions are evidence of local mixed mode condition along the front of the fatigue crack while the tensile mode I area in the middle of the specimen corresponds to a plane strain conditions. The shear lips development on the specimen surface becomes more intensive during the second zone of fatigue crack growth when the fatigue striation process in the central zone of the fracture surface becomes dominant. Under conditions of stationary loading a transition to the second zone of crack growth is related to a decrease in crack growth acceleration which is because of changes in damage accumulation process near the crack tip. The main hypotheses of modern fracture theories are associated with a concept of a critical distance considered as the fundamental characteristic setting interrelation between the processes occurring on both micro - and macrolevel with respect to material structure. This critical distance is often identified with the fracture process zone (FPZ) size where microdamages accumulates until crack growth takes place at the macroscopic scale level. The size of FPZ, as it is established by Shlyanikov (4), is parameter sensitive to change of the size of a specimen and its loading conditions. With the help of the FPZ-concept it is possible also to describe well known scale effect at fracture.

In the present work a comparison of experimental data of crack growth rate with the theoretical prediction is made and on this basis the influence of the inherent stress biaxiality on the characteristics of crack growth in specimen two geometries is estimated.

Theoretical Procedures

Well known that the specimen thickness play a key role in characterizations of the crack-tip fields as it depends on distance to the tip and the free edge-surface of the specimen. With reduction of thickness of the cracked body of a fracture condition vary from plane strain up to plane stress with occurrence of mixed modes at appearance of shear lips (Fig. 1). Although the stress intensity factor K has been tabulated for a wide range of geometries, the biaxiality parameter B is only available for a more limited number of cases. Larsson and Carlsson (3) have demonstrated that the B has a significant effect on the shape and size of the plastic zone which develops at the crack tip. In front of a stable growing crack are realised the small-scale yielding conditions (SSYC). Therefore we shall consider an opportunity of determination of plastic zone at SSYC with taking into account of influence of inherent stress biaxiality.

Shape and size of the plastic zone

For a strain-hardening material for which the uniaxial stress-strain relation may be written as

$$\frac{\varepsilon}{E\sigma_0} = \left(\frac{\sigma}{\sigma_0}\right)^n \quad (1)$$

the distribution of strain in the plastic zone can be obtained using the Makhutov model (5), i. e.

$$\varepsilon_p = K_\varepsilon \varepsilon_n$$

Where σ_0 - yield stress; $\varepsilon_n, \varepsilon_p$ - nominal and plastic strain intensity respectively, K_ε - strain concentration factor, n - strain hardening exponent. Here

$$K_\varepsilon = (\varepsilon_{el})^{P_\varepsilon} / \sigma_n \quad (2)$$

and ε_{el} - elastic stress intensity at the crack tip. Substituting equation (2) into (1) we obtain

$$\varepsilon_p = \frac{2(1+\nu)}{3E} (\sigma_{el})^{P_\varepsilon} \quad (3)$$

where

$$P_\varepsilon = \begin{cases} P_\varepsilon^{2D} = \frac{2n-0,5(n-1)(1-\bar{\sigma})}{n+1} & \text{- for plane stress} \\ P_\varepsilon^{3D} = \frac{2n-0,5(n-1)(1-\bar{\sigma}\sqrt{1+\nu(\nu-1)})}{n+1} & \text{- for plane strain} \end{cases}$$

To take advantage of a equation (3) it is necessary to determine the singularity stress intensity $\bar{\sigma}_{el} = \sigma_{el}/\sigma_0$. For the plane stress

$$(\bar{\sigma}_{el}^{2D})^2 = \bar{\sigma}_{xx}^2 + \bar{\sigma}_{yy}^2 - \bar{\sigma}_{xx}\bar{\sigma}_{yy} + 3\bar{\sigma}_{xy}^2 \quad (4)$$

and for the plane strain

$$(\bar{\sigma}_{el}^{3D})^2 = \frac{1}{2} \left[(\bar{\sigma}_{xx} - \bar{\sigma}_{yy})^2 + (\bar{\sigma}_{yy} - \bar{\sigma}_{zz})^2 + (\bar{\sigma}_{zz} - \bar{\sigma}_{xx})^2 + 6\bar{\sigma}_{xy}^2 \right] \quad (5)$$

where $\bar{\sigma}_{zz} = \nu(\bar{\sigma}_{xx} + \bar{\sigma}_{yy})$. From the analyses of Rice (1) follows that

$$\begin{bmatrix} \bar{\sigma}_{xx} & \bar{\sigma}_{xy} \\ \bar{\sigma}_{xy} & \bar{\sigma}_{yy} \end{bmatrix} = \frac{\bar{K}}{\sqrt{2\pi r}} \begin{bmatrix} f_{xx}(\theta) & f_{xy}(\theta) \\ f_{xy}(\theta) & f_{yy}(\theta) \end{bmatrix} + \begin{bmatrix} \bar{T} & 0 \\ 0 & 0 \end{bmatrix} \quad (6)$$

The magnitude of the nonsingular term $\bar{T} = T/\sigma_0$ is defined through a biaxiality parameter B , introduced by Leever and Radon (2)

$$\bar{T} = \frac{BK}{\sqrt{\pi a}} = \bar{\sigma} B \left(\frac{a}{w}\right) Y\left(\frac{a}{w}\right) \quad (7)$$

where $Y(a/w)$ - geometric factor of specimen for K. Replacing σ_{ii} in equation (3) by $\bar{\sigma}_{ii}$ and substituting equations (4-7) into it, one can calculate distributions of dimensionless elastic-plastic strain intensities $\varepsilon_p/(E\sigma_0)$. For this effect we shall substitute equations (4-7) into (3) and obtain equations for r_p/a which permits one to determine the shape and size of the plastic deformation zone:

the plane stress

$$\left(\frac{r_p^{2D}}{a}\right) = \left[\frac{P_a}{-P_a \pm \sqrt{P_a^2 - 2P_a \left\{ 2B^2 - \frac{2}{(\bar{\sigma}Y)^2} \left[\frac{3\bar{\varepsilon}_p}{2(1+\nu)} \right]^{2/p_s^{2D}} \right\}}} \right]^2 \quad (8)$$

$$P_a = 2(f_{xx}^2 + f_{yy}^2 + f_{xx}f_{yy} + 3f_{xy}^2); P_s = \sqrt{2}B(2f_{xx} - f_{yy})$$

the plane strain

$$\left(\frac{r_p^{3D}}{a}\right) = \left[\frac{P_a}{-P_b \pm \sqrt{P_b^2 - 2P_a \left\{ 2B^2(1-\nu+\nu^2) - \frac{2}{(\bar{\sigma}Y)^2} \left[\frac{3\bar{\varepsilon}_p}{2(1+\nu)} \right]^{2/p_s^{3D}} \right\}}} \right]^2 \quad (9)$$

$$P_a = 2 \left[(f_{xx} + f_{yy})^2 (1 - \nu + \nu^2) - 3f_{xx}f_{yy} + 3f_{xy}^2 \right];$$

$$P_a = \sqrt{2}B \left[2(f_{xx} + f_{yy})(1 - \nu + \nu^2) - 3f_{yy} \right]$$

and

$$f_{xx}(\theta) = \cos \frac{\theta}{2} \left(1 - \sin \frac{\theta}{2} \sin \frac{3\theta}{2} \right); f_{yy}(\theta) = \cos \frac{\theta}{2} \left(1 + \sin \frac{\theta}{2} \sin \frac{3\theta}{2} \right);$$

$$f_{xy}(\theta) = \sin \frac{\theta}{2} \cos \frac{\theta}{2} \cos \frac{3\theta}{2}$$

In Fig.2 the computational elastic-plastic boundary curves are shown at $\bar{\varepsilon}_p = \varepsilon_p / (E\sigma_0) = 1$ for different variants of stress-strain state. It is seen that the elastic-plastic boundary size depends essentially on the inherent stress biaxiality factor B. The more complete estimation of influence B can be obtained from comparison of the plastic zone sizes on the free surface and middle plane of specimen respectively. Well know that the specimen thickness play a key role in characterisations of the crack-tip fields and is dependent on distance to the tip and free edge-surface of the specimen. Assumed that the countour of plastic zone local to the crack tip have shape as it is shown in Fig. 3 . Where t is thickness of cracked body and both r_p^{2D} and r_p^{3D} are the plastic zone sizes on the free surface and middle plane. The coordinates of points (A and B) of transition from plane strain up to plane stress are set by value $0,5 r_p^{2D} / t$ which is in turn connected to the width of shear lips on a failed specimen surface. We shall consider change of the ratio r_p^{2D} / r_p^{3D} with take info account B depending on dimensionless crack length (a/w) . In the present work we focus the analysis on specimens of two geometries - single-edge-notched specimen (SENS) and compact tension specimen (CTS). On the basis of numerical results by Lewers and Radon (2) the dependence B from (a/w) one can approximate by the following equations for a specimen of each geometry

$$B\left(\frac{a}{w}\right) = 1.537\left(\frac{a}{w}\right)^{2.1} - 0.5 \quad - \text{ SENS}$$

$$B\left(\frac{a}{w}\right) = 0.304 \ln\left(\frac{a}{w}\right) + 0.768 \quad - \text{ CTS} \quad (10)$$

The expressions for geometric factor of specimen $Y(a/w)$ are well known in the literature on the fracture mechanic

$$Y\left(\frac{a}{w}\right) = 1.12 - 0.23\left(\frac{a}{w}\right) + 10.55\left(\frac{a}{w}\right)^2 - 21.72\left(\frac{a}{w}\right)^3 + 30.39\left(\frac{a}{w}\right)^4 \quad \text{- SENS}$$

$$Y\left(\frac{a}{w}\right) = \frac{\left[2 + \left(\frac{a}{w}\right)\right] \left[0.886 + 4.64\left(\frac{a}{w}\right) - 13.32\left(\frac{a}{w}\right)^2 + 14.72\left(\frac{a}{w}\right)^3 - 5.6\left(\frac{a}{w}\right)^4\right]}{\left[1 - \left(\frac{a}{w}\right)\right]^{3/2} \left[\pi\left(\frac{a}{w}\right)\right]^{1/2}} \quad \text{- CTS (11)}$$

Displayed in Fig. 4(a) to (b) are the variations of the ratio r_p^{2D}/r_p^{3D} taking into account of equations (10,11) as a function of dimensionless crack length (a/w) . Note that r_p^{2D}/a and r_p^{3D}/a are given, respectively, in equations (8) and (9). The effect of stress biaxiaality for a specimen each geometry increases with increase of applied nominal stresses $\bar{\sigma}$.

Local fracture stress

Let $\bar{\sigma}_f = \sigma_f/\sigma_0$ makes sense local fracture stress along of crack front. Its distribution on thickness of a cracked body in general case it is not known. For the purpose of the present analysis accepted the distribution on thickness of local fracture stress $\bar{\sigma}_f$ along of crack front in a qualitative meaning repeats the behaviour of the plastic zone size as it is shown in Fig. 3. Then

$$\frac{\bar{\sigma}_f^{2D}}{\bar{\sigma}_f^{3D}} = \frac{r_p^{2D}}{r_p^{3D}} \quad (12)$$

From this equation follows that on the free surface of the specimen

$$\bar{\sigma}_f = \bar{\sigma}_f^{2D} \quad \text{for } z/h = 1 \quad (\text{plane stress})$$

and

$$\bar{\sigma}_f = \bar{\sigma}_f^{3D} \text{ for } 0 \leq z/h \leq A \text{ (plane strain)} \quad (13)$$

Where h - half-thickness of the specimen. The distribution of the $\bar{\sigma}_f$ on a site of crack front from point A (the coordinate of transition from the plane strain up to the plane stress) up to free surface of the specimen can be given by the following equation

$$\bar{\sigma}_f = \bar{\sigma}_f^{3D} \left(\frac{r_p^{2D}}{r_p^{3D}} \right) \left\{ 1 - \frac{1 - (r_p^{3D} / r_p^{2D})}{(r_p^{2D} / 4h)} \sqrt{\left(1 - \frac{z}{h} \right) \left[2 \left(\frac{r_p^{2D}}{4h} \right) + \frac{z}{h} - 1 \right]} \right\} \quad (14)$$

where $\bar{\sigma}_f^{3D} \approx \bar{\sigma}_u^{true} = \sigma_u / \sigma_0 (1 - \psi)$ - is the true ultimate tensile stress and ψ - is reduction of area. The order of determination of the ratio r_p^{2D} / r_p^{3D} is discussed above.

Fracture process zone size

Determination of the fracture process zone was made by application of the strain energy density criterion by Sih (6). A critical distance r_c ahead of the crack tip is assumed to take place when the strain energy density in an element reaches certain critical value. A relative FPZ size $\bar{\delta} = r_c / a$ was introduced by Shlyannikov (4)

$$\bar{\delta}_c = \left\{ \frac{\bar{S}_2 \pm \left[\bar{S}_2^2 - 4(\bar{W}_c^* - \bar{S}_3)(\bar{S}_1 + \bar{S}_p) \right]^{1/2}}{2(\bar{W}_c^* - \bar{S}_3)} \right\}^2 \quad (15)$$

where

$$\bar{W}_c^* = \left(\frac{\sigma_0}{\sigma} \right)^2 \left[\frac{1}{2} \bar{\sigma}_f^2 + \frac{m}{n+1} \bar{\sigma}_f^{n+1} \right] \quad (16)$$

Here $\bar{S}_i = (i = 1, 2, 3)$ and \bar{S}_p are elastic and plastic strain energy density factors respectively which are given by as

$$\begin{aligned}\bar{S}_1 &= 0.25(1+\nu)(\kappa-1)Y^2 & \bar{S}_2 &= 0.5(1+\nu)(1-\kappa)BY^2/\sqrt{2} \\ \bar{S}_3 &= 0.125(1+\nu)(\kappa+1)B^2Y^2 & \bar{S}_p &= \frac{n\lambda}{n+1} \frac{\pi}{I_n} \tilde{\sigma}^{n+1} Y^2\end{aligned}$$

$\lambda = 1, \kappa = (3-\nu)/(1+\nu)$ - plane stress $\lambda = 1-\nu^2, \kappa = 3-4\nu$ - plane strain

It should be noted that distinctions between plane strain and plane stress are defining not only κ values but both HRR - field parameters $\tilde{\sigma}(n, \theta)$ and I_n corresponding to each stress-strain state type. The local fracture stress $\bar{\sigma}_f$ in equation (16) is given by equation (14).

Crack growth rate model

Making use of the cyclic stress and strain curve described by the parameters $\sigma_f^*, \varepsilon_f^*$ and n^* which have the same interpretation as the static stress-strain curve. A critical state of elastic-plastic hysteresis loop can be written in terms of the strain energy density as

$$\left(\frac{d\bar{W}}{dV}\right)_c = 4\sigma_f^* \varepsilon_f^* (2N_f)^{-m} \quad (17)$$

Application of equation (17) leads to relation for fatigue damage in the fracture process zone

$$\frac{da}{dN} = 2\bar{\delta}\alpha \left[\frac{\sigma^2 \bar{S}_f - \sigma_{th}^2 \Delta S_{th}}{4\sigma_f^* \varepsilon_f^* E \bar{\delta}} \right]^{1/m} \quad (18)$$

where N-number of cycles of loading, σ_{th} and ΔS_{th} - threshold values of nominal stress and strain energy density factor. Here $\bar{S}_f = \bar{S}_1 + \bar{S}_p + \sqrt{\bar{\delta}} \bar{S}_2 + \bar{\delta} \bar{S}_3$. The parameter m in equation (18) may be expressed in term of the cyclic strain hardening exponent n^* as $m = (1+n^*)/(5+n^*)$. The FPZ- size in equation (18) is given by equation (15). The work by Shlyannikov (4) contain more details about determination of the crack growth rate equation (18).

Results and discussion

The theoretical approach elaborated in present work was used to describe and computational estimations of the crack growth rate for two different type of specimens: single-edge-notched specimen (SENS) and compact tension specimen (CTS). Three different types of heat treatment are administered to the 30 Cr steel resulting in the different microstructures referred to as steel A, B and C. The main mechanical and fracture properties of the 30Cr steel are given in Table 1.

Table 1. Mechanical and fracture properties of 30Cr-steel type A,B and C

Steel type	σ_o (MPa)	σ_u (MPa)	σ_{II}^{true} (MPa)	$\left(\frac{dW}{dV}\right)_c$ (MPa)	K_{Ic} (Mpa /m)	ψ (%)	n	$\frac{\sigma_{II}^{true}}{\sigma_o}$	$\bar{\varepsilon}_f$
A	1514	1750	2333	23.67	76.8	25	7.79	1.541	0.288
B	1039	1136	2064	26.34	159.6	45	6.42	1.987	0.599
C	444,8	761.2	1438	12.55	101.4	65	4.3	3.232	0.635

Experimental background of theoretical model

Displayed in Fig.5(a) to (c) are the variations of the crack growth rate as a function of material properties. Note that theoretical predictions are given by equations (7-16) and (18) which taking into account inherent stress biaxiality. These experimental and theoretical results are presented for the SENS geometry loaded by $\bar{\sigma} = 0.0165, 0.0181$ and 0.0351 for 30Cr steel A, B and C respectively. It can be seen that the agreement between experimental and theoretical data is good.

Analysis of scale effect

The influence of the sizes of a specimen is a well-known phenomenon in the experimental fracture mechanics. The aquations (7-18) allow to estimate influence of stress biaxiality parameter B on crack growth rate. Parameter B belongs to the characteristics stress-strain state therefore it the influence is realized though a fracture process zone where takes place the accumulation of damage ahead of the fatigue crack.

Figs.6 and 7 shows the increase of the crack growth rate with increase of specimen width w . Three sets of curves are given for each of the two specimen types SENS (Fig.6) and CTS (Fig.7). For the 30Cr steel A, B and C da/dN increased moderately exhibiting the so called "scale effect" at fatigue fracture. The data on Figs.6 and 7 corresponds to a computed results by equation (18). It is apparent that crack growth rate would depend not only on specimen type but also on specimen width and/or crack size. It is possible to notice that then more sizes of a specimen that more distinction in crack growth rate in specimens of the various geometries.

Shear lips on fatigue crack surfaces

Is mentioned earlier that formation shear lips results in occurrence of mixed modes fracture on a specimen surface. For fatigue crack growth the shear lip width is approximately equilly to coordinate of the transition from plane strain up to plane stress. The equation (15) allows to receive the crack front form along thickness of a specimen through the appropriate FPZ sizes at various stages cyclic fracture. Note that this equation takes into account also influence of inherent stress biaxiality parameter B .

Presented in Fig.8(a) to (d) are plots of normalized FPZ size δ/a versus the normalized specimen thickness z/h for the SENS made of 30 Cr steel C. Equations (7,10) and (15) are used for evaluating B and hence $\bar{\delta}$. Three sets of curves are given for each combination of the specimen width and thickness; they correspond to $a/v=0.3, 0.4$ and 0.5 . All specimen subjected by cyclic load $\bar{\sigma}=0.17$. As it follows from Fig.8 crack front form, and hence, shear lip sizes are dependent from the specimen sizes at the same values of relative crack length. It can be seen that the greatest influence of inherent stress biaxiality parameter B takes place on a free surface of a specimen.

Because of distinctions at FPZ sizes for $B=0$ and $B \neq 0$ it is necessary to expect various values of crack growth rate accordingly for $B=0$ and $B \neq 0$. Influence of inherent stress biaxiality on crack growth rate will be more essential at increase level of applied nominal stress $\bar{\sigma}$. Especially sensitive to change of parameter B will be, as expected, crack growth rate of physically short cracks because in this case $\bar{\delta} = \delta/a \approx 1$ and the influence of the nonsingular term T dependent from B becomes more significant.

References

- (1) RICE J.R., (1974), Limitations to the small scale yielding approximation for crack tip plasticity, *J. Mech. Phys. Solids*, vol.22, pp.17-26.
- (2) LEEVERS P.S. and RADON J.C., (1982), Inherent stress biaxiality in various fracture specimen geometries, *Int.J.Fract.*, vol.19, pp.311-325.
- (3) LARSSON S.G. and CARLSSON A.J.,(1973), Influence of non-singular stress term and specimen geometry on small-scale yielding at crack tip in elastic-plastic materials, *J.Mech.Phys.Solids*, vol. 21, pp.263-277.
- (4) SHLYANNIKOV V.N., (1996), Modelling of crack growth by fracture damage zone, *Theoret. Appl. Fract. Mech.*, vol. 25, pp. 187-201.
- (5) MAKHUTOV N.A., (1981), Deformation criteria of fracture and calculation elements structure strength, Mashinostroenie Press, Moscow.
- (6) SIH G.C., (1973), Some basic problems in fracture mechanics and new concepts, *Engng. Fract. Mech.*, vol. 15 pp. 365-377.

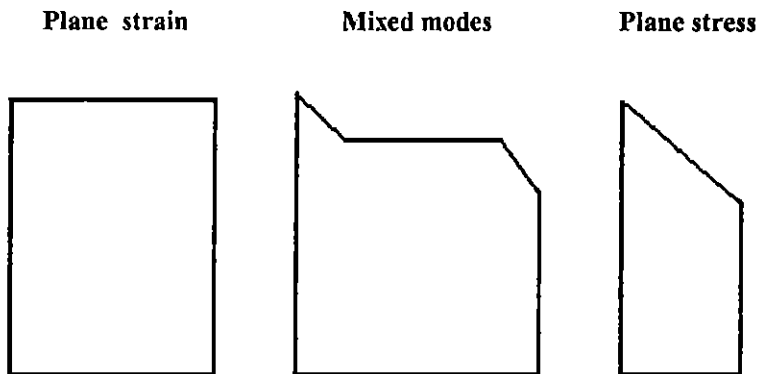


Fig.1 Types of fracture

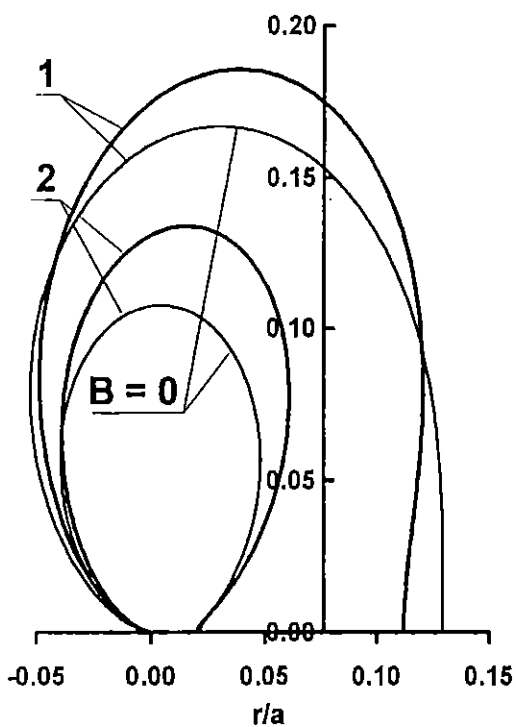


Fig.2 Plastic zone for plane stress (1) and plane strain (2) $n=13$, $\nu=0.3$, $\bar{\sigma}=0.3$, $a/w=0.35$

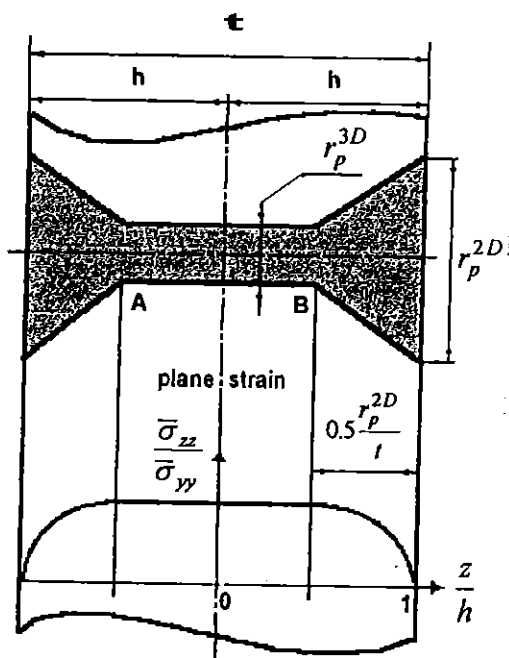


Fig.3 Schematic illustration of the plastic zone ahead crack tip

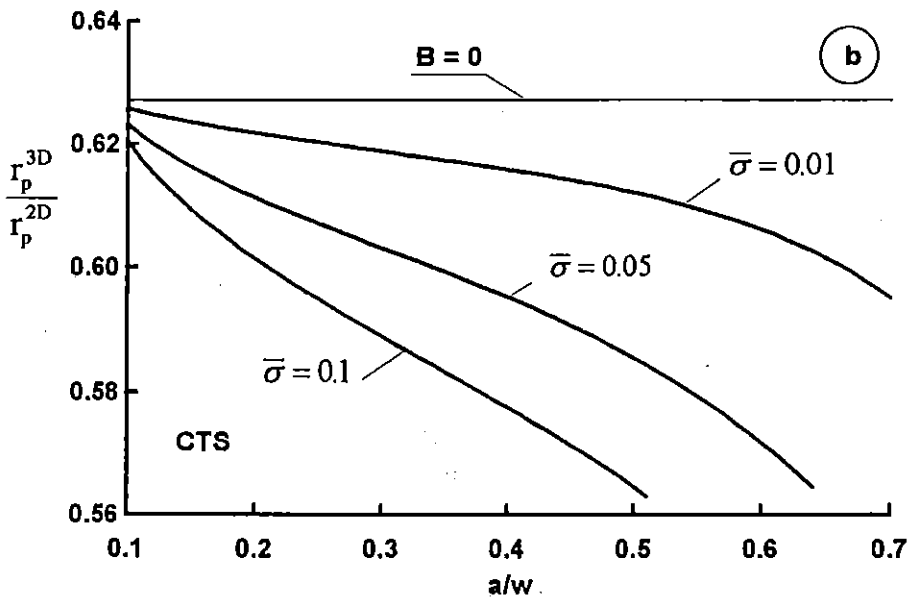
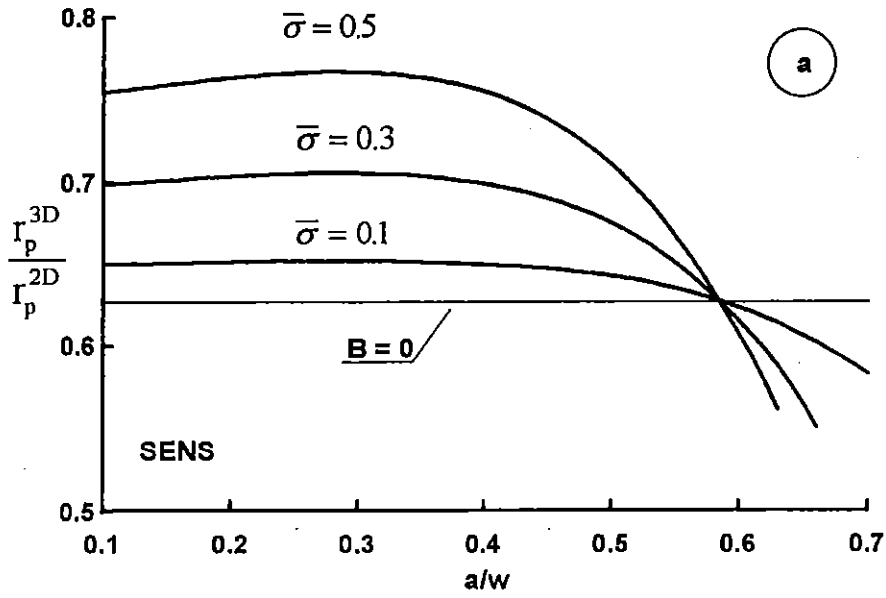


Fig.4 Range of change dimensionless plastic zone size ratio in various specimen geometries

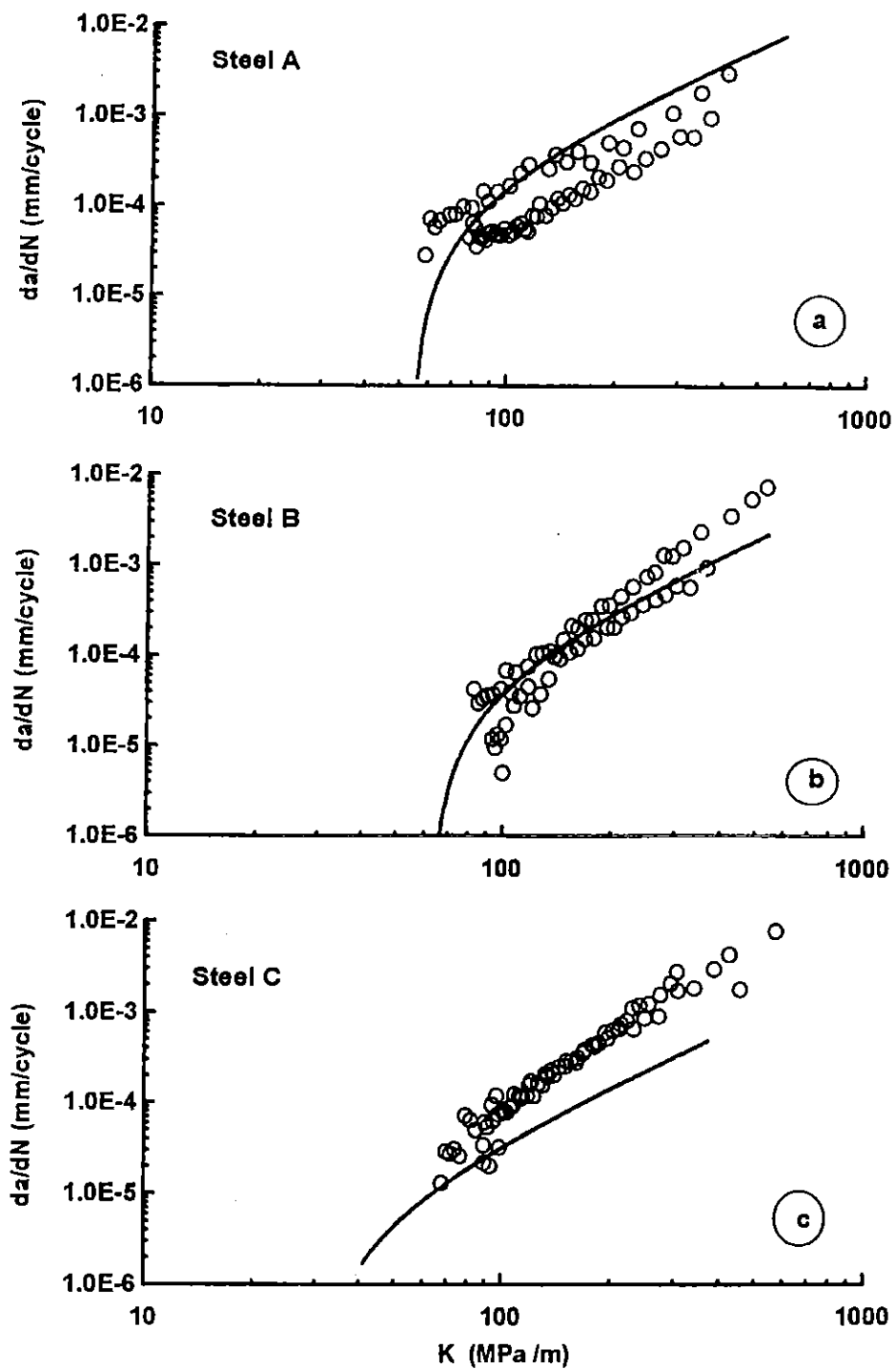


Fig.5 Comparison between the theoretical predictions and experimental data for SENS

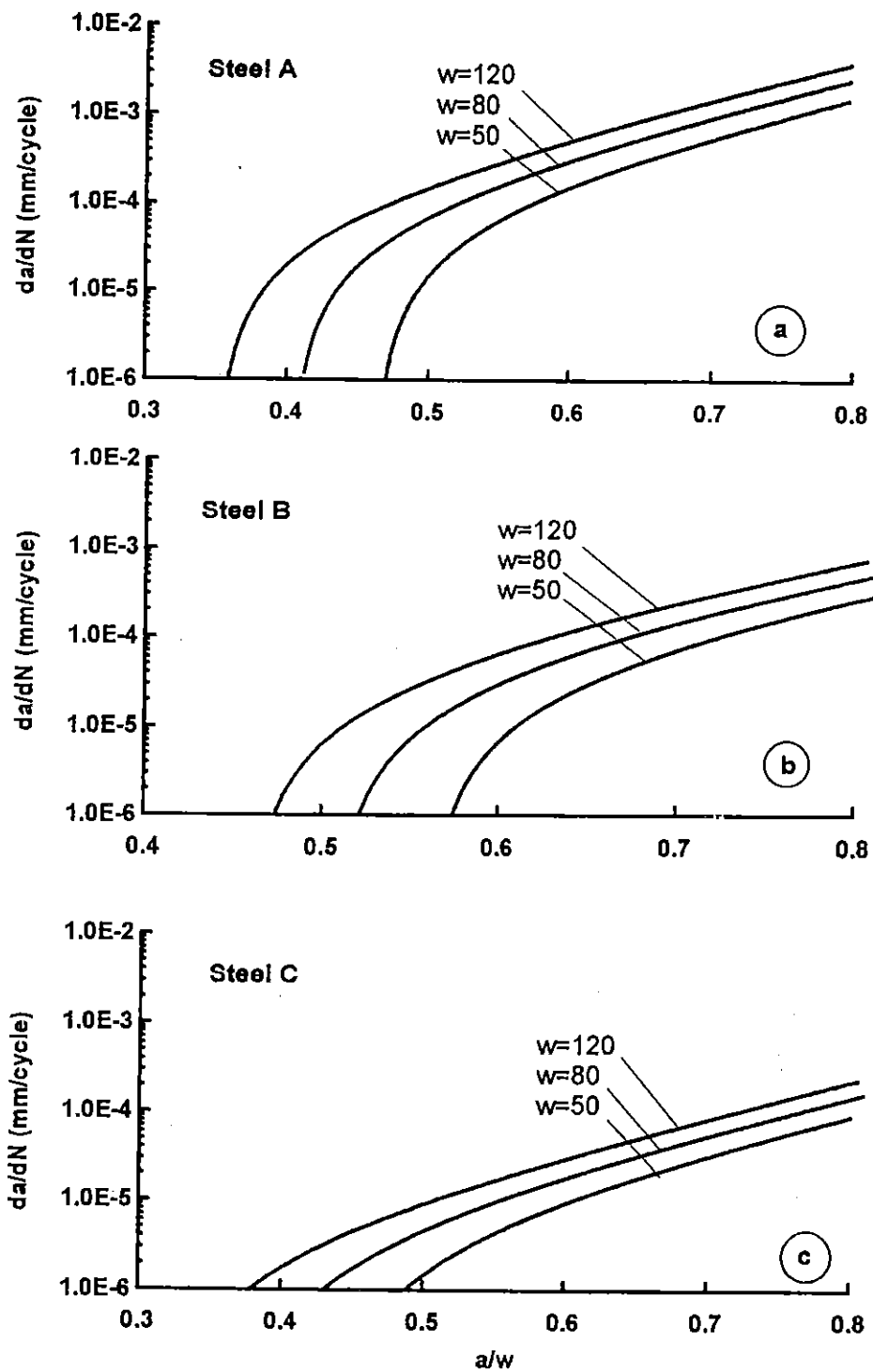


Fig.6 Scale effect in SENS geometry

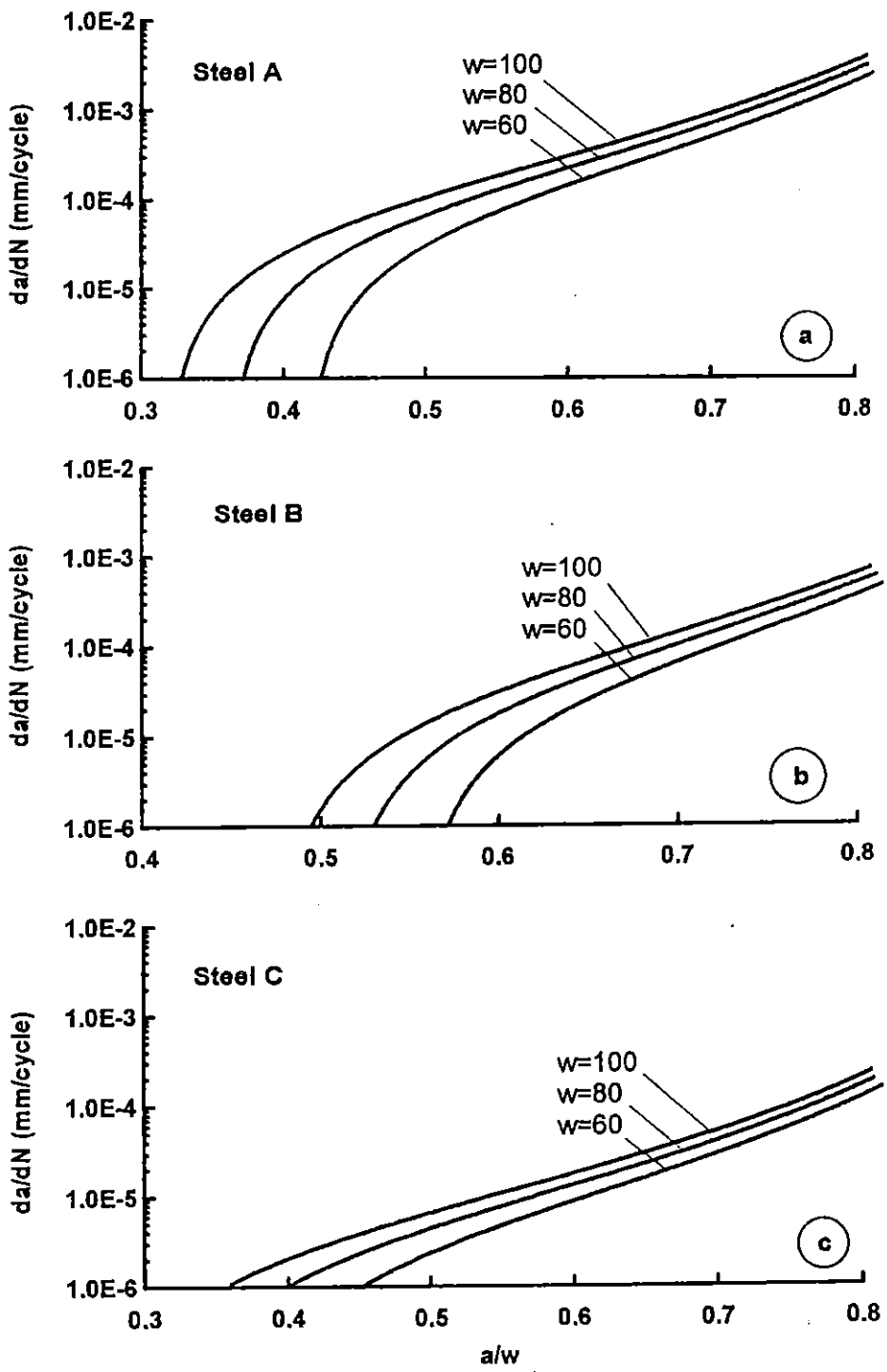


Fig.7 Scale effect in CTS geometry

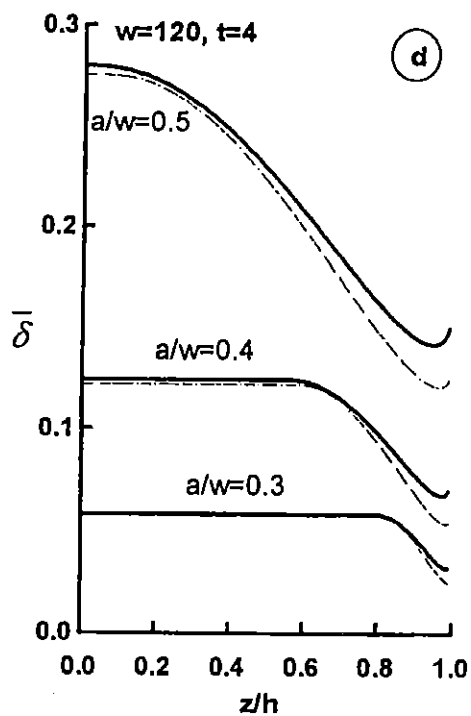
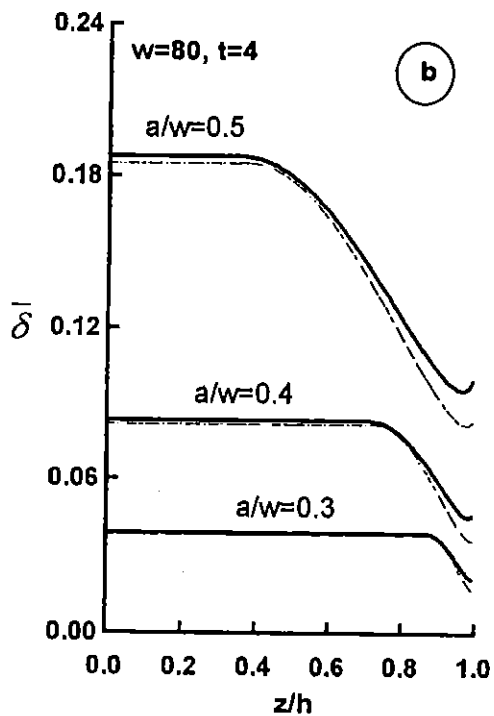
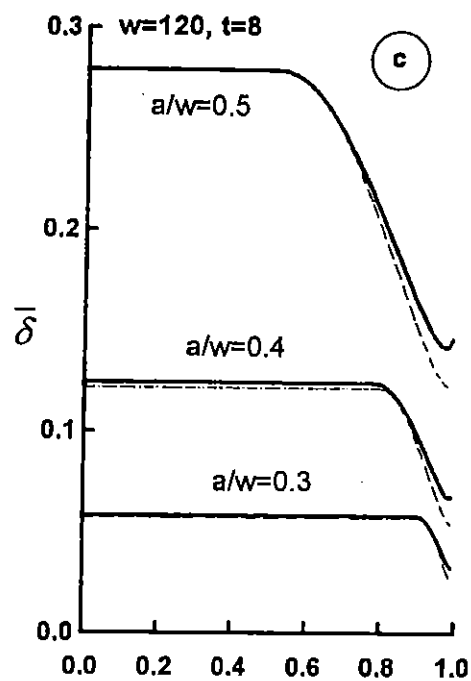
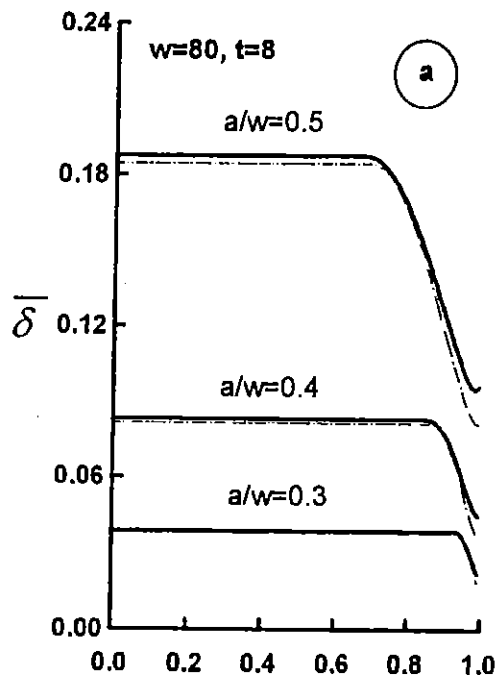


Fig.8 Fatigue crack front form for various width and thickness of the SENS geometry (dashes line - $B=0$)